Flexoskeleton Fingers: 3D Printed Reconfigurable Ridges Enabling Multi-functional and Low-cost Underactuated Grasping

Qifan Yu, Mingsong Jiang, and Nick Gravish

***Abstract*—In this letter we present a design and fabrication framework for soft, underactuated grippers that utilize reconfigurable laminate layers for finger stiffness modulation. The grippers consist of internal flexoskeleton layers, which are hybrid soft-rigid structures composed of a flexible thermoplastic sheet with rigid structures 3D printed directly onto the flexible layer. The flexoskeleton structures are encased in an external silicone skin, which enables smooth and soft contact surfaces between the gripper and objects. We designed the flexoskeleton layers to be reconfigurable through layer sliding, which enables finger stiffness modulation by two methods: 1) continuum stiffness modulation through layer sliding to enable strong overlap gripping, and 2) locking and unlocking of flexoskeleton ridge structures that enable stable grasps without actuation. The gripper designs presented here are extremely easy to design and fabricate and present a template for future soft grippers.**

***Index Terms*—Soft Robot Materials and Design, Underactuated Robots, Grippers and Other End-Effectors**

I. Introduction

UNDERACTUATED grippers present an appealing option for grasping, in which complex objects can be grasped through passive mechanical interaction of the hand with objects. Because of the passive compliance and low number of actuators, underactuated grippers can grasp a wide range of objects with simple control inputs [1], [2]. Recent advances in the design, materials, fabrication, and control of continuum soft robots have enabled new approaches to generate compliant underactuated grippers [3], [4], [5].

Soft-robotic grippers have often taken the form of pneumatically actuated cylinders fabricated from cast silicone [6], [7], [8] or fabric [9], [10]. Soft grippers offer promising grasping abilities thanks to their inherent compliance and continuum actuation. With some additional features and modifications such as programmed chamber sizes [6] or bio-mimetic shapes [11], soft grippers can grasp a variety of objects with considerable lifting force [6]. However, traditional pneumatic grippers often require precise fabrication of the encasing skin and fingers to ensure air-tight seals and uniform rigidity [12]. These pneumatic grippers are often sensitive to wear and puncture when handling objects. Furthermore, the fabrication of traditional pneumatic gripper's entirely soft body and its air-tightness prevent easy reconfiguration of the gripper itself, since reconfiguration of the mold requires recasting [13]. This raises the manufacturing cost, causes significant delays, and makes online reconfiguration of the gripper challenging.

An exciting direction in soft robotics is modularity and reconfiguration of body structure during usage [14], [15]. For examples, dual-stiffness structures such as sliding layer laminates (SLLs) [16], [17] and origami jamsheets [18] have enabled stiffness modulation in thin structures; variable stiffness mechanisms such as shape memory alloy (SMA) stiffness modulation [19], [20], sliding layer mechanism [21] have been incorporated into soft robots to realize multi-state locomotion. For underactuated soft grippers, reconfigurable mechanisms can be an effective paradigm to enable variable grasping forces and finger geometry within a single soft gripper [22]. For examples, grippers demonstrated in [23], [24], [25] are able to vary the finger stiffness through reconfiguration or input force modulation. As a result of stiffness modulation, these grippers are able to grasp objects with larger contact area, larger gripping force, and controllable finger curvature.

A recently developed hybrid method for 3D printing rigid material onto flexible sheets—flexoskeleton printing [26]—has been developed by these authors. The flexoskeleton process enables inherently flexible mechanisms to be printed on a standard (and low cost) rigid filament fused deposition modeling (FDM) 3D-printer. Rigid filaments are bonded to a flexible thermoplastic sheet during the printing process enabling flexibility from the flexible base layer and rigidity from the filament. Thus, the flexoskeleton process enables a wide control of geometry and rigidity through the FDM printer capabilities. The ease of use and modularity of this process make it an appealing template upon which to create reconfiguring soft grippers.

In this paper, we introduce an underactuated soft gripper made of 3D printed flexoskeleton with reconfigurable ridges and cast silicone skin, as shown in Fig. 1(a). This gripper has two fingers, each made of a 3D-printed flexoskeleton inner structure and encased in a silicone shell as the skin. A 3D-printed palm connects the fingers and a tendon is routed through both fingers and connected to a central pulley and motor to achieve passive compliance and underactuation. The gripper without any reconfiguring mechanism (the default gripper) is able to generate as large as 12N of lifting force with

Manuscript received: October, 23, 2020; Revised January, 11, 2021; Accepted February, 16, 2021.

This paper was recommended for publication by Editor Kyu-Jin Cho upon evaluation of the Associate Editor and Reviewers' comments. This work was supported by the National Science Foundation under Grant No. (1935324).

All authors are with the Mechanical & Aerospace Engineering Department, University of California, San Diego. (email {qyu@, mij032@eng., ngravish@eng.} ucsd.edu).

Digital Object Identifier (DOI): see top of this page.

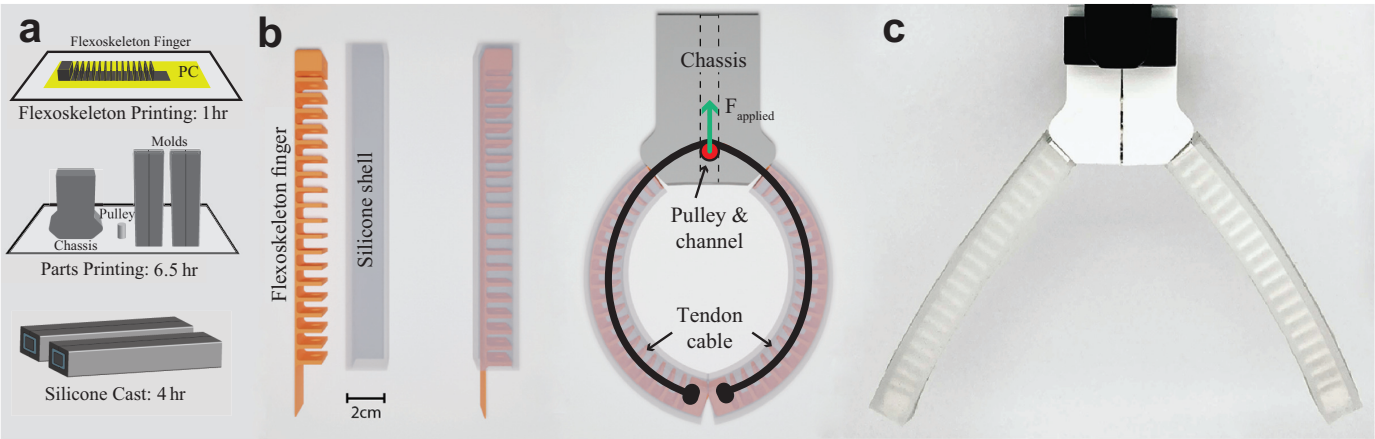

Fig. 1. Overview of the default gripper with no reconfiguring mechanism: (a) fabrication of gripper components, (b) rendered design of components and the assembled default gripper showing underactuated tendon and pulley mechanism, (c) a prototype of the assembled default gripper.

just one stepper motor, and is able to grab a variety of objects. We introduce a variable stiffness sliding layer mechanisms and a hyperextension grasping mode respectively to enable grasp reconfiguration. Through these mechanisms, the stiffness of the gripper can be modulated to achieve multi-state grasping, and locked ridges can enable high gripping forces without actuation. As a result of these two reconfigurable mechanisms, the gripper is able to produce lifting forces twice as large as the default gripper and achieves better conformability over a broad sets of objects.

II. Design

A. Fabrication

All grippers presented in this paper utilize a common set of design and fabrication methods. The grippers are composed of two main elements, a flexoskeleton inner structure with sliding layers and tendon guides, and a soft silicone exterior. Flexoskeleton structures are generated from a recently developed 3D printing method, which enables rapid fabrication of rigid-flexible structures [26]. We use a Prusa i3 MK3S FDM 3D printer to 3D print an array of rigid vertical ridges (Polylactic acid; PLA filament) atop a heated thermoplastic sheet (Polycarbonate; PC) as shown in Fig. 1(a). The thermoplastic sheet (PC) is adhered to the heated bed with double-stick tape prior to the printing process. When the PC layer is heated to 80-95°C, we observe extremely strong adhesion between the rigid PLA print material and the flexible PC layer (peel strength as large as 15 N/cm [26]). In addition, flexoskeleton components are capable of repeated deformation without significant degradation when the PLA base layer is less than 1 mm [26]. The flexoskeleton printing process allows us to design gripper components that are inherently flexible with rigid structural support, tendon guides, and ridge locking mechanisms from the rigid PLA. Furthermore, the bending stiffness of the flexoskeleton fingers can be precisely controlled by the PLA layer thickness.

The flexoskeleton fingers begin with a base layer of PLA, which is printed entirely over the PC surface. This base layer provides stiffness and support to the flexoskeleton structure. Atop this layer we print a row of vertical ridges that have three functions: 1) they provide structural support to the soft silicone outer layer, 2) they limit the maximum curvature of the finger at prescribed angles, and 3) they provide a tendon guide for actuation. Other components of the gripper are printed from standard rigid 3D printing processes and take only hours to be printed, including sliders, silicone molds, gearbox, and gears for reconfiguring mechanisms. Lastly, we cast a silicone skin using Dragonskin 20 as the soft and compliant exterior. The silicone skin is cast using a 3D printed mold and a stick with rectangular cross section. We do not cast the flexoskeleton finger directly into the silicone mold and instead treat it as a replaceable and reusable silicone skin. A summary of the gripper components are shown in Table I, as well as in Fig. 1(a). The top three components in Table I are used in all grippers while the bottom three components are introduced in later sections for gripper reconfiguration.

The default gripper design with no reconfigurable mechanisms is shown in Fig. 1(b-c). A 2 mm thick silicone shell encases each flexoskeleton finger, which have rigid rectangular ridges in order to increase both the overall bending stiffness of the finger and to support the silicone skin. Since we aim to create the default gripper with fingers that can curve into any shapes, the rectangular ridge that does not jam until large angle deflection is used, so no jamming is observed throughout

TABLE I
Summary of fabrication process of all parts of grippers. Components above the horizontal line indicate default gripper components. Below horizontal line are modifications for stiffness changing or locking grippers.

Part	Material	Method	Time
Palm/Chassis and pulley	PLA	3D printing	2.5 hr
2 Molds	PLA	3D printing	4 hr
Silicone skins	Dragonskin 20	Casting	4 hr
2 Flexoskeleton Fingers	PLA+PC	3D printing	1 hr
Gearbox and gears	PLA	3D printing	1.5 hr
Slider for sliding	PLA+PC	3D printing	20 min
2 sliders for locking	PLA+PC	3D printing	30 min

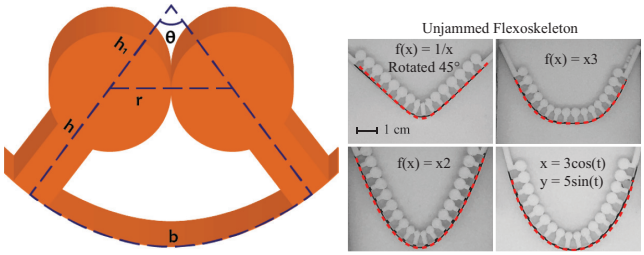

Fig. 2. Flexoskeleton ridges enable control of maximum bending curvature of the finger. (a) Schematic of two jammed round ridges and their parameters when jammed. (b) Examples of controlled curvature in flexoskeleton ridges. The red dashed curves show the prescribed curvature function and the experimental realization.

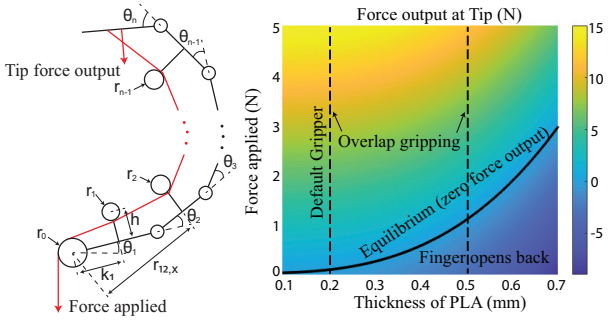

Fig. 3. Force output at tip of the finger. The relation between force output and actuation force are linear. The black line is the equilibrium point where output forces are zero, meaning the finger is at equilibrium.

experiments. A gripper unit consists of two fingers that are inserted into a 3D-printed chassis, which serves as the palm of the gripper. A single tendon is connected between the end of each finger and routed across a single pulley, which is connected to a stepper-motor to actuate both fingers. The tendon connecting the two fingers is routed through holes printed into the vertical ridges of the flexoskeleton layer and terminated at the end of fingers, as shown in Fig. 1(b). The tendon is actuated by displacing the pulley, and this mechanism realizes both passive compliance and underactuation [1]. Tendons are Power Pro Fiber Braided fishing line.

After the components are printed, the assembly of the gripper takes less than 20 minutes and does not require significant assembly hardware. Note that printing and assembling of a default gripper takes less than 8.5 hours using only one FDM 3D printer, however this process can be sped up with multiple printers, while all components are reusable. The total cost of raw materials for the default gripper is less than $5.00 ($1.50 2 cast silicone shells, $1.25 3D-printed palms and pulley, $0.50 2 3D-printed flexoskeleton fingers, $1.50 3D-printed molds).

The entire process does not require human intervention except at the beginning of casting and the assembly. Thanks to the gripper's modular design, the fabrication and reassembly of modified fingers takes less than 1.5 hours after the first printing, since the silicone skins, palm and molds are all reusable. Furthermore, all components of the gripper are tolerant to failure thanks to the robustness of the flexoskeleton printing [26].

B. Modeling

To inform our design geometry and aid our analysis, we present here two mathematical models for flexoskeleton grippers.

1) Curvature control through ridge jamming: The vertical structures (ridges) of the flexoskeleton fingers enable grasp force distribution through the silicone skin, but they also act as joint stops for the fingers. To derive the stopping angle of the fingers as a function of ridge geometry, we derive the relationship between the ridge geometry and the jamming angle. This relationship is governed by simple equation generated from the geometry of jammed ridges [26]:

$$\theta r = (b - \theta h)\sin\left(\frac{\theta}{2}\right) \tag{1}$$

The arc length of the curved finger b, the radius of the ridge r, and the height of the ridge h, govern the maximum bend angle (θ). The parameters are illustrated in Fig. 2(a).

With a desired curvature of the finger, the round ridges can be designed using specified b, r, h to create joint limits that prevents over-curved finger flexion and to design grasp profiles for specific object categories. The round ridges are especially important on fingers, in which reconfigurable sliding layer mechanisms enable high-curvature grasps during an overlap grip. In Fig. 2(b), we show the comparison between our model generated curvature and that observed in experiment. We observe very good agreement between the observed and desired curvature (shown in red dashed lines) of our flexoskeleton structures.

2) Finger Force Modeling: To understand the grasp force capabilities of our fingers and to appropriately determine the flexoskeleton layer thickness, we employ a simple model of tendon-actuated fingers. We treat each middle point of two ridges as a joint, and the other sections as rigid links. The force of the finger can be modeled as a function of both the stiffness of the finger "joints" and the actuation force by equating the input and output virtual power during quasi-equilibrium states [1]:

$$\mathbf{J^T f} = \mathbf{T^{-T} t} \tag{2}$$

Where $\mathbf{J}$ is the Jacobian of the finger, $\mathbf{f}$ is the force output of each phalange, $\mathbf{T}$ being the transmission matrix of the tendon-drive actuation, and $\mathbf{t}$ being the input torque at each joint. Assuming there is no friction, The flexoskeleton finger is equivalent to the Da-Vinci tendon-driven finger [1], in which case the transmission matrix $\mathbf{T}$ and Jacobian $\mathbf{J}$ can both be calculated, knowing the length of each phalange and height of each ridge. The equations that derive these matrices can be found in [1].

In our flexoskeleton finger, we treat each flexure between the vertical ridges as a revolute joint. The stiffness of these joints is determined by the bending stiffness of a uniform cantilever beam assuming small angle deflection (less than 10°). The curvature of the finger is assumed to be a 60° uniform arc. As a result, the relation between the thickness of PLA backing layer, force applied to the pulley and the force output at each

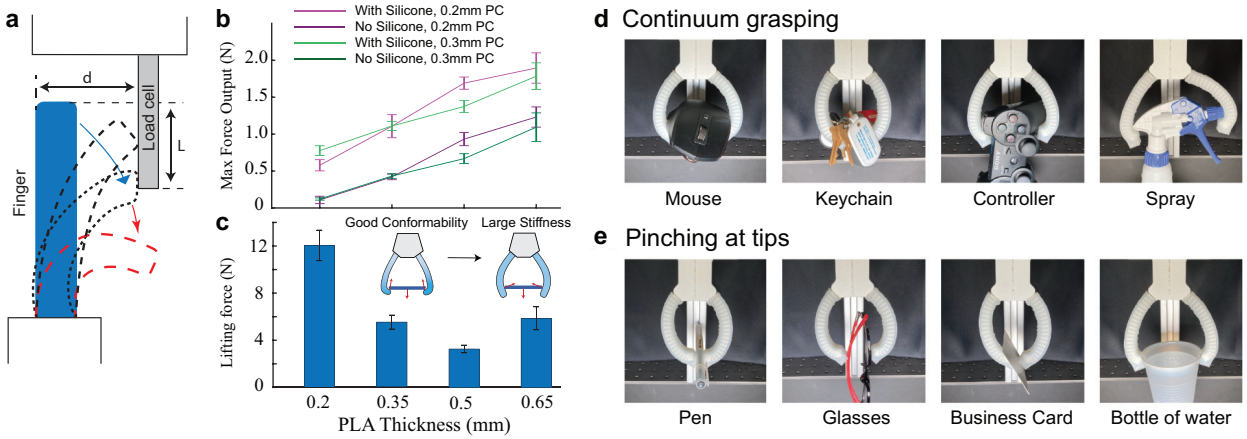

Fig. 4. (a). Experimental setup for finger force testing. The finger bends to the right and pushes against the load cell until the finger slips by. (b). Maximum finger tip force during gripper actuation as a function of PLA layer thickness. 10 trials are conducted on each finger. (c) Maximum lifting force of two-finger gripping as a function of PLA layer thickness. Bars are mean and standard deviation from 10 trials. (d-e) Application examples of object grasping in free space. (d) Continuum grasping of objects with wide contours. (e) Objects with low aspect-ratio are pinched by the gripper tips.

joint can be found from Eqn. 2. The force output at the tip of finger under these setting is plotted in Fig. 3.

III. Performance of Default Grippers

We perform three experiments to characterize the stiffness, maximum lifting force, and conformability of our default flexoskeleton grippers without reconfigurable capabilities. Since the purpose of these experiments is to characterize a default gripper without tunable conformability, we choose to use rectangular ridges, so no local finger stiffening occurs throughout the experiments. Meanwhile, these experiments will serve as a metric for comparison with the reconfigurable mechanisms introduced in the next section. The ridge profiles of the default gripper are uniform with parameters b = 5 mm, h = 9 mm, r = 0 mm (rectangular ridges).

We tested the tip-force generation of a single finger in a load-displacement experiment (Fig. 4(a)). The finger is mounted on a fixed chassis, and a tendon is shortened by a stepper motor. A load cell is placed at a distance d = 60 mm from the backing layer of the finger, and the end of the finger is L = 40 mm from the top of finger. The finger will push the load cell with a maximum force immediately before the finger slips through the contact and passes the load cell. The maximum tip force is measured on individual fingers with flexoskeleton base layers ranging from 0.2 to 0.65 mm, with and without the silicone skin. The maximum force measured by the load cell shows a linear relation with the thickness of the PLA backing layers, as presented in Fig. 4(b). However, the thickness of the backing PC layer does not have significant effect on the force output. The force output significantly increased with the silicone skin, which indicates the importance of friction in the tip force output in this experiments.

We next measure the lifting ability of the complete two-finger gripper as a function of PLA thickness layer (Fig. 4(c)). We actuate and hold the tendon through a motorized linear stage. The gripper grasps onto a 70mm wide rectangle between the two fingers. This object keeps the contact area and position of the initial grasp constant. We then add weights of increasing mass until eventually the gripper is unable to provide enough lifting force, and the load object fell through. The maximum lifting forces for fingers of different thickness are measured to characterize their ability to lift heavy objects.

Our results from single finger tip, and two finger grasping forces present conflicting results. In single finger experiments, the output tip force increased linearly with flexoskeleton stiffness (PLA thickness), as shown in Fig. 4(b). However, in lifting experiments the peak force of the fingers with 0.5 mm thick backing is approximately 4 times smaller than for those with 0.2 mm thickness backing layer, as shown in Fig. 4(c). This contradiction is because when the weight is applied, the thinner flexoskeleton grippers are able to bend inward, forming a caging curvature and increasing lift strength (shown in Fig. 4(c)). As a result, fingers having thinner backing are able to provide more upward normal force when lifting the load objects of our experiment. In contrast to the beneficial effect of tip curvature from low thickness PLA layers, high stiffness (thicker PLA) flexoskeleton layer grippers also exhibited increasing lifting force. For fingers with a thicker flexoskeleton base layer, the actuation force produces large frictional force against the object, which results in larger lifting forces. Consequently, when the thickness of PLA backing is 0.65 mm, the lifting force rises due to an increase in fingers' gripping force, as shown in Fig. 4(c).

We then perform grasping tests with common objects that have complex and distinct contours to evaluate the gripper's grasping performance. We use a default gripper with 0.2 mm backing layer fingers since they have the best conformability and largest lifting force. During the test, the objects are placed in between two fingers as the gripper closes. Fig. 4(d-e) shows a few gripping experiments performed. In general, the presented grasping tests can be characterized into two modes, depending on the object characteristics. For wide contour objects, the entirety of fingers are able to conform around objects and provide enough lifting force with low pressure as in Fig. 4(d); for narrow or high-aspect ratio profile objects, the gripper is able to pinch the objects at its tips as in Fig. 4(e).

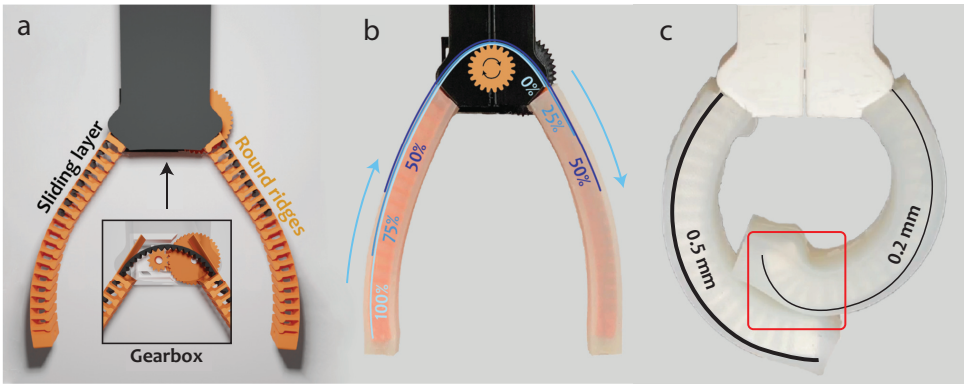

Fig. 5. A reconfigurable gripper with a sliding layer mechanism. (a) The flexoskeleton structure and the sliding layer (black layer) gearbox and actuator. The sliding layer in the default position is at 50% extension in both fingers. When it is displaced to one of the fingers the differential stiffness between fingers changes and overlap gripping is enabled. (b) A photo of the gripper with the layer alignment percentage shown in different configurations. (c) An overlap grip (red rectangle) can be achieved when the outer finger has the stiffer layer, while the inner finger has a thinner layer thickness.

IV. Reconfigurable Mechanisms

While the default grippers explored in the previous section provide high force and are compatible with a wide array of objects, we now seek to explore the reconfigurable capabilities of flexoskeleton grippers. We integrate two separate reconfigurable mechanisms that can be easily customized and fabricated: 1) a sliding layer mechanism that enables differential stiffness modulation, and 2) a ridge locking mechanism that locks both fingers in a closed configuration. These mechanisms both enable multi-state grasping through modulation of stiffness and kinematic motion of flexoskeleton fingers. The following section illustrates how these modulations enable improved lifting performance and additional grasping modes, expanding the potential use of flexoskeleton grippers.

A. Variable Stiffness Sliding Layer Mechanism

In the default gripper, the two fingers are actuated through a differential mechanism with a single pulley, and thus the sequence of finger closing in the absence of contact should be symmetric. However, if we can modulate the differential stiffness of the fingers, then under the same input actuation, the finger having lower stiffness will deform and close more than the stiffer finger. In this section, a method that modulates the passive differential stiffness of the two fingers is implemented by selectively sliding a stiffening flexoskeleton layer to one of the two fingers, thus inducing a differential stiffness between fingers.

To produce a variable stiffness change in the finger, we incorporate a 3D-printed 0.8 mm thick sliding layer into the 0.2mm backing layer finger. The sliding layer is printed using the flexoskeleton process and serves as a flexible rack, with PLA teeth printed atop the flexible thermoplastic sheet(PC). A rectangular hole within the ridges forms a central channel that enables free translation of the sliding layer along the length of the fingers. The flexoskeleton ridges here serve multiple purposes: 1) they provide structural support for the silicone skin, 2) they limit finger bending through jamming, and 3) they enable free movement of the sliding layer within the central channel in the ridges. By varying the sliding layer displacement between the fingers, the stiffness differential of opposing fingers can be continuously modulated. The flexoskeleton slider is printed as a flexible rack and a complementary pinion is attached to a gearbox with gear ratio of 1.86, which is ultimately connected to a servo motor (Inset in Fig. 5(a)). Once again, the flexoskeleton printing process enables easy fabrication of the flexible rack and pinion mechanism in less than 2 hours.

In Fig. 5(a), we show the flexoskeleton sliding mechanism within the fingers and the actuator within the chassis of the gripper. Layer sliding is driven by a servo motor, and the sliding layer is able to slide in between both fingers, modulating the stiffness differential as follows: the stiffness difference between two fingers is maximum when the sliding layer is at 0% or 100% of one finger (measured as fraction of finger length), while the stiffness is balanced when the sliding layer is at 50% layer displacement. As a result, this reconfigurable gripper is able to perform overlap grips and symmetric grasping according to the position of the sliding layer. As an example of the extreme capabilities of differential stiffness, we show an overlap grip in Fig. 5(c). We hypothesize that in addition to the substantial increase in lifting force, the new grasping mode—overlapping grip—will enable firm grasping for smaller objects. This accommodation for the geometry of objects by adding only one degree of freedom (one servo motor) is an approach for soft fingers similar to the joint angle stiffness control for rigid fingers. The added grasping mode, however, is a novel path of variable stiffness mechanism, absent in most variable stiffness gripper such as [23], [24], [25].

We first characterize the increase in the finger tip force that results from layer sliding in a single flexoskeleton finger. A single silicone-encased flexoskeleton finger with a sliding layer inserted (Fig. 6(a)) is used to perform the same gripping force experiment. With the same setup conducted for the default gripper, we now vary the percent of layer inserted instead of varying the backing layer thickness. As the result, the gripping force increase observed was more than twice as large as the minimum stiffness (0% inserted sliding layer), as shown in Fig. 6(a). The gripping force difference between the left and right fingers is then calculated from these experiments and is presented in Fig. 6(b).

Next, we test the hypothesis that overlapping grasps enable larger lifting force from the two-finger gripper. We perform maximum lifting force experiments using a rectangular block and incremental loading as described in the default gripper section. A maximum lifting force of 21N is observed in the overlap gripping mode, which is almost twice as large

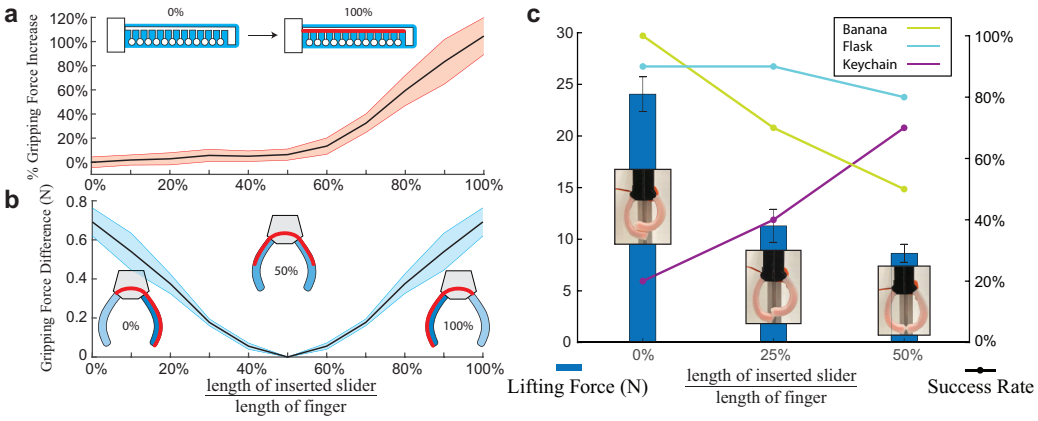

Fig. 6. Gripping force performance of the sliding layer gripper. (a) Normalized gripping force increase compared to gripping force with no inserted sliding layer, which is 0.66 N. (b) Gripping force difference of left and right fingers as the sliding layer slides in between. Large difference implies overlap gripping. (c) Lifting performance and grasping success rate of the gripper with the sliding layer mechanism. 0% implies no insertion into the right finger, while 50% implies symmetric setup of gripper.

as the maximum lifting force for symmetric configurations (Fig. 6(c)). The overlap gripping mode has a much larger lifting force compared to the symmetric gripper. We hypothesize that grasp reconfiguration enables different shapes and loads of objects to be held. We tested three objects with distinct characteristics: 1) object with medium radius (flask: 56g, ⌀5.4cm), 2) object with small radius and unbalanced weight (banana: 165g, ⌀3.5cm), and 3) a narrow object with low profile (keychain: 70g). The success rate of grasping a banana and keychain, as shown in Fig. 6(c), differs significantly from the overlap to symmetric grasping modes. This suggests the overlap gripping mode performs better for small and round objects by conforming their narrow shape better. The symmetric mode performs well for objects with low profile and unbalanced weight by pinching. Both modes performs well for relatively large and round objects.

B. Hyperextension Motion and Ridge Locking Mechanisms

In this last section, a different method of reconfiguration is explored, where a sliding flexoskeleton layer is used to lock the fingers in a closed state through jamming of the flexoskeleton ridges (Fig. 7(a)-(d)). This grasping method requires that the unactuated state of the gripper be in the closed position (which in previous sections had to be actuated to be achieved). Thus, we design our silicone skin such that the resting configuration is in the fingers closed position. Thus, the silicone skin provides a resisting elastic force to gripper opening. We use tendon-actuated hyperextension of the fingers to open the grasp, elastic restoring force of the skin to close the grasp, and a ridge locking mechanism to lock the grasp for high lifting force production.

Inspired by granular jamming that stiffens the finger and provides larger lifting force [23], we propose a ridge locking mechanism to achieve high grasp forces through locking of flexoskeleton ridges. The curved silicone with thickness of 2 mm causes the fingers to passively close around grasps with a neutral radius of 20 mm. The mold and the cured pre-curved silicone shell is shown in Fig. 7(e). This arc-shaped silicone shell is chosen because when installed, 1) this silicone shell has an end that curves up, so when holding an object the fingers form a caging shape that provides significant upward normal force; 2) the root of this silicone shell is perpendicular to the chassis, so the root of flexoskeleton fingers inside are not bent there. Since the default dynamic grasping state is closed, the fingers now have to be actuated to open. To achieve hyperextension actuation, the flexoskeleton ridges face away from the grasp direction, shown in Fig. 7(a), so the tendon through ridges provides moment that opens up the finger. Hyperextension actuation and ridge locking enable the gripper to grasp objects without power input; its gripping force comes completely from the deformation of curved silicone skins (note there is no differential actuation in this motion).

As shown in Fig. 7(b), an asymmetric ridge profile with parameters $b = 5$ mm, $h = 9$ mm is introduced on the flexoskeleton finger, along with a lower ridge profile with parameters $b = 5.2$ mm, $h = 5$ mm on a flexoskeleton slider that slides inside the finger. Both ridge profiles are constructed by using two 45 degree angled segments with two circular caps on each end, as shown in Fig. 7(c). The flexoskeleton ridges are similar to the sliding layer design, in which a central channel enables layer sliding. The ridges are locked when tendon 1 pulls the slider in between the flexoskeleton finger, and unlocked when tendon 2 is pulled, as presented in Fig. 7(c). This locking mechanism is incorporated with hyperextension motion but not the previous two, because it will stiffen the finger when bent in the ridge direction, but not bending in the PC layer direction. A concept hyperextensive gripper with this ridge locking mechanism is shown in Fig. 7(a) and the locking flexoskeleton layers are photographed in Fig. 7(b). Note that only the front half of the finger is needed to be unlocked for the gripper to open to release objects.

With this hyperextension and ridge locking design, fingers are able to be locked in the curved grasping configuration, which is expected to increase the grasping force. The control sequence of the gripper involves: 1) actuation of the hyperextension tendon to open up the grasp, 2) releasing the hyperextension tendon to close the grasp, and 3) actuation of locking tendon (tendon 2) to lock the grasp. When the grasp is to be released, we actuate an antagonistic tendon that releases the locking (Fig. 7(d)). Thus, the ridge locking grippers require a main actuator to open and close the grasp and additional actuators to open and close the ridge locking mechanism.

To examine the grasping capabilities of ridge locking fingers, we measured the force-displacement of individual fingers. A constant displacement motion is applied to the finger, which

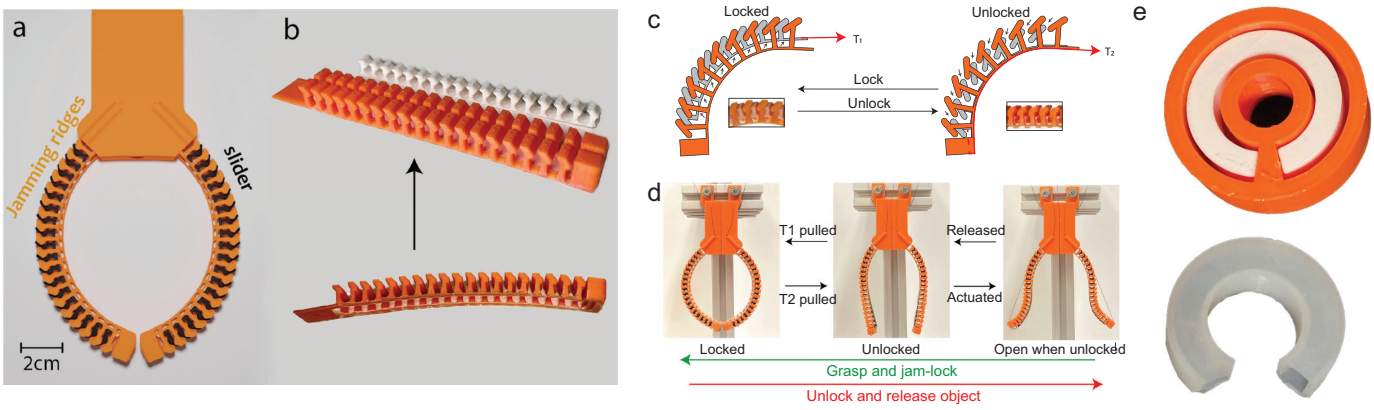

Fig. 7. Reconfigurable Hyperextensive gripper (a) in a rendered setup without silicone skin and (b) its printed flexoskeleton finger and slider, both having asymmetric ridges. (c) ridge locking mechanism through tendons that reconfigure slider under the bridges of finger, and (d) control sequence among locked, unlocked, and unlocked and opened without silicone skins. (e) shows the mold used for casting curved silicone shell and the cured shell. The mold contains a outer casing as well as a curved stick with rectangular cross section, both of which are 3D printed. The silicone shell is trimmed to fit the length of flexoskeleton finger after cured.

acted against a load cell. The load cell generated an opening force against the grasp, and the blocking force of the load-cell is measured during pullout (Fig. 8(a)). The reaction forces of unlocked and locked fingers are plotted in Fig. 8(b). With the ridge locking mechanism enabled, the blocking force of the finger reaches almost three times the blocking force of the unlocked finger when displaced 2 cm from their equilibrium. The locking takes effect on the stiffness of the finger when it is displaced around 0.8 cm, from which point the stiffness of the locked finger increases and deviates from that of the unlocked finger. Thus, the ridge locking effect requires modest displacement to be engaged. This makes sense since the locking effect is not induced by any external pressure, but instead it is a result of grip loading, causing the finger to displace and engage ridge locking.

To evaluate the grasping performance of ridge locking fingers, the lifting force of a two-finger gripper is measured by establishing a grasp between the gripper and a circular test-load. We increase the load until eventually the grasp failed and the load slipped through the fingers. A significant increase in lifting force is observed from the ridge-locked fingers as shown in Fig. 8(c). The ridge locking gripper is capable of a lifting force as large as the force from the actuated default gripper with 0.2 mm backing layer fingers.

To examine the effect of ridge jamming on grasp success rate, we examined the lifting performance of a ridge locking gripper lifting a round object with relatively large radius and mass (776.7g, ⌀7.5cm). When the ridge locking is not engaged, the gripper has a low success rate of lifting and grasping; however, consistent with our force measurements, the gripper with ridge locking engaged has a high success rate (Fig. 8(c)). Compared to the default gripper, the ridge jamming design is actuated in hyperextension and is capable of almost as large a lifting force as the default gripper. Actuation through hyperextension may be well suited to grasping delicate objects since the grasping force is provided by the passive elasticity of the skin. However, actuation through hyperextension is also a limitation of this design in that grasp force cannot be controlled, potentially limiting the range of object shapes that can be grasped.

V. Conclusions

This paper presents an underactuated robotic gripper that uses sliding-based reconfiguration that can change grasping modes through differential stiffening or ridge locking. A new fabrication process, flexoskeleton printing [26], is central to the rapid and easy fabrication of hybrid flexible and rigid structures. Flexoskeleton printing enables precise control of rigid material geometry deposited (and securely bonded) to a flexible thermoplastic backing layer. Gripper design and fabrication using these methods can be accomplished in short time and uses low-cost 3D printers and materials.

To explore the capabilities of flexoskeleton printed fingers we developed several implementations of underactuated grippers capable of: 1) default symmetric grasping, 2) overlap grasping through differential stiffness, and 3) ridge locking hyperextension grasping. Each design has its own advantages and disadvantages. The gripper with a central sliding layer mechanism is more suitable when target objects have relatively large geometry variation as this system can change gripping configuration. The overlap gripping mode is able to handle objects that are heavy (as large as 24N), small, or thin in cross section, and the symmetric grasping mode is able to handle objects that are flat (near 2D geometry) or large (more than 100 mm long), etc. However, the gripper with ridge locking is more suitable when target objects are delicate, since grip closure is not actuated by tendon; instead, the grasping force comes entirely from the passive stiffness of the material and the ridge jamming. This means the object will not be squeezed or pinched with force more than necessary for holding the object.

In the current implementation, these two reconfiguring mechanisms can not be combined into a single gripper. However, in this study we have introduced and explored the capabilities of flexoskeleton based grippers and future implementations may be able to combine multiple capabilities from

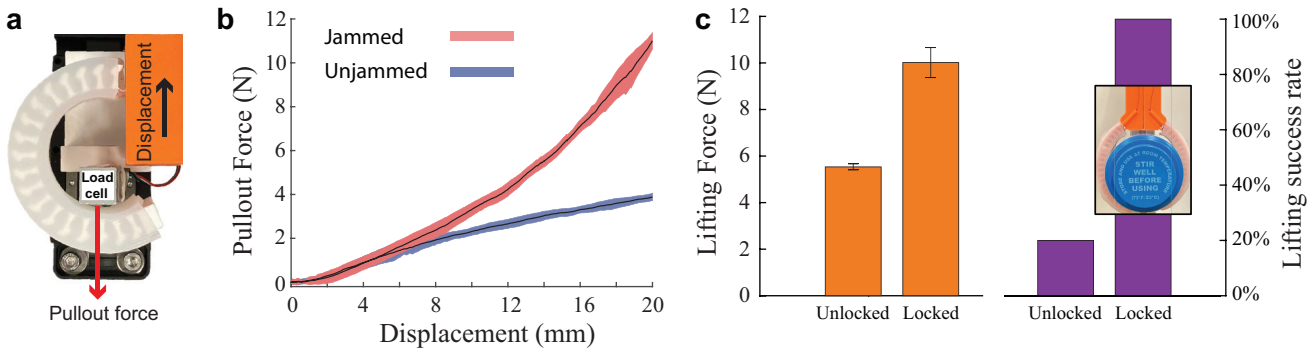

Fig. 8. (a) Image of blocked-force measurement of pullout force on a locked gripper. (b) Blocking force measurement of finger with ridge locking mechanism. 10 trials are conducted for both configurations. (c) Lifting performance and grasping success rate for reconfigurable hyperextensive gripper. 10 trials are conducted for both lifting force and success rate measurement

these designs. We envision that the versatility of flexoskeloton printing will enable a diversity of future grippers using 3D printed, compliant mechanisms.

ACKNOWLEDGEMENT

This material is based upon work supported by the National Science Foundation under Grant No. (1935324).

REFERENCES

[1] Lionel Birglen, Thierry Laliberté, and Clément M Gosselin. *Underactuated robotic hands*, volume 40. Springer, 2007.

[2] Lael U Odhner, Leif P Jentoft, Mark R Claffee, Nicholas Corson, Yaroslav Tenzer, Raymond R Ma, Martin Buehler, Robert Kohout, Robert D Howe, and Aaron M Dollar. A compliant, underactuated hand for robust manipulation. *Int. J. Rob. Res.*, 33(5):736–752, April 2014.

[3] Luc Marechal, Pascale Balland, Lukas Lindenroth, Fotis Petrou, Christos Kontovounisios, and Fernando Bello. Toward a common framework and database of materials for soft robotics. *Soft Robotics*, 2020.

[4] Jun Shintake, Samuel Rosset, Bryan Schubert, Dario Floreano, and Herbert Shea. Versatile soft grippers with intrinsic electroadhesion based on multifunctional polymer actuators. *Advanced Materials*, 28(2):231–238, 2016.

[5] Wei Wang and Sung-Hoon Ahn. Shape memory alloy-based soft gripper with variable stiffness for compliant and effective grasping. *Soft robotics*, 4(4):379–389, 2017.

[6] Paul Glick, Srinivasan A Suresh, Donald Ruffatto, Mark Cutkosky, Michael T Tolley, and Aaron Parness. A soft robotic gripper with gecko-inspired adhesive. *IEEE Robotics and Automation Letters*, 3(2):903–910, 2018.

[7] Raphael Deimel and Oliver Brock. A novel type of compliant and underactuated robotic hand for dexterous grasping. *The International Journal of Robotics Research*, 35(1-3):161–185, 2016.

[8] Jianshu Zhou, Shu Chen, and Zheng Wang. A soft-robotic gripper with enhanced object adaptation and grasping reliability. *IEEE Robotics and automation letters*, 2(4):2287–2293, 2017.

[9] Loai AT Al Abeach, Samia Nefti-Meziani, and Steve Davis. Design of a variable stiffness soft dexterous gripper. *Soft robotics*, 4(3):274–284, 2017.

[10] Yanqiong Fei, Jiangbei Wang, and Wu Pang. A novel fabric-based versatile and stiffness-tunable soft gripper integrating soft pneumatic fingers and wrist. *Soft robotics*, 6(1):1–20, 2019.

[11] N Giri and I Walker. Continuum robots and underactuated grasping. *Mechanical Sciences*, 2(1):51–58, 2011.

[12] Jianglong Guo, Khaled Elgeneidy, Chaoqun Xiang, Niels Lohse, Laura Justham, and Jonathan Rossiter. Soft pneumatic grippers embedded with stretchable electroadhesion. *Smart Materials and Structures*, 27(5):055006, 2018.

[13] Jiawei Zhang, Andrew Jackson, Nathan Mentzer, and Rebecca Kramer. A modular, reconfigurable mold for a soft robotic gripper design activity. *Frontiers in Robotics and AI*, 4:46, 2017.

[14] Zhongdong Jiao, Chen Ji, Jun Zou, Huayong Yang, and Min Pan. Vacuum-powered soft pneumatic twisting actuators to empower new capabilities for soft robots. *Advanced Materials Technologies*, 4(1):1800429, 2019.

[15] Matthew A Robertson and Jamie Paik. New soft robots really suck: Vacuum-powered systems empower diverse capabilities. *Science Robotics*, 2(9), 2017.

[16] Yong-Jai Park, Jong-Gu Lee, Sangwon Jeon, Heejin Ahn, Jesung Koh, Junghyun Ryu, Maenghyo Cho, and Kyu-Jin Cho. Dual-stiffness structures with reconfiguring mechanism: Design and investigation. *Journal of Intelligent Material Systems and Structures*, 27(8):995–1010, 2016.

[17] Mingsong Jiang and Nick Gravish. Sliding-layer laminates: a robotic material enabling robust and adaptable undulatory locomotion. In *2018 IEEE/RSJ International Conference on Intelligent Robots and Systems (IROS)*, pages 5944–5951. IEEE, 2018.

[18] Jifei Ou, Lining Yao, Daniel Tauber, Jürgen Steimle, Ryuma Niiyama, and Hiroshi Ishii. jamsheets: thin interfaces with tunable stiffness enabled by layer jamming. In *Proceedings of the 8th International Conference on Tangible, Embedded and Embodied Interaction*, pages 65–72, 2014.

[19] Shixin Mao, Erbao Dong, Hu Jin, Min Xu, Shiwu Zhang, Jie Yang, and Kin Huat Low. Gait study and pattern generation of a starfish-like soft robot with flexible rays actuated by smas. *Journal of Bionic Engineering*, 11(3):400–411, 2014.

[20] Yuuta Sugiyama and Shinichi Hirai. Crawling and jumping of deformable soft robot. In *2004 IEEE/RSJ International Conference on Intelligent Robots and Systems (IROS)(IEEE Cat. No. 04CH37566)*, volume 4, pages 3276–3281. IEEE, 2004.

[21] Kevin C Galloway, Jonathan E Clark, Mark Yim, and Daniel E Koditschek. Experimental investigations into the role of passive variable compliant legs for dynamic robotic locomotion. In *2011 IEEE International Conference on Robotics and Automation*, pages 1243–1249. IEEE, 2011.

[22] Mariangela Manti, Vito Cacucciolo, and Matteo Cianchetti. Stiffening in soft robotics: A review of the state of the art. *IEEE Robotics & Automation Magazine*, 23(3):93–106, 2016.

[23] Kaori Mizushima, Takumi Oku, Yosuke Suzuki, Tokuo Tsuji, and Tetsuyou Watanabe. Multi-fingered robotic hand based on hybrid mechanism of tendon-driven and jamming transition. In *2018 IEEE International Conference on Soft Robotics (RoboSoft)*, pages 376–381. IEEE, 2018.

[24] Amir Firouzeh and Jamie Paik. An under-actuated origami gripper with adjustable stiffness joints for multiple grasp modes. *Smart Materials and Structures*, 26(5):055035, 2017.

[25] Elizabeth Fox and Frank L Hammond III. Soft variable stiffness joints for controllable grasp synergies in underactuated robotic hands. In *2020 3rd IEEE International Conference on Soft Robotics (RoboSoft)*, pages 586–592. IEEE, 2020.

[26] Mingsong Jiang, Ziyi Zhou, and Nicholas Gravish. Flexoskeleton printing enables versatile fabrication of hybrid soft and rigid robots. *Soft Robotics*, 2020.